catalysts

MDPI

Article

Development of an Environment-Friendly and Electrochemical Method for the Synthesis of an Oxadiazole Drug-Scaffold That Targets Poly(ADP-Ribose)Polymerase in Human Breast Cancer Cells

Sindhu M. Parameshwaraiah [1], Zhang Xi [2], Akshay Ravish [1], Arunkumar Mohan [1], Vanishree Shankarnaik [3], Dukanya Dukanya [1], Shreeja Basappa [4], Habbanakuppe D. Preetham [1], Ganga Periyasamy [3], Santhosh L. Gaonkar [5], Peter E. Lobie [2,6,7], Vijay Pandey [6,7,*] and Basappa Basappa [1,*]

1 Laboratory of Chemical Biology, Department of Studies in Organic Chemistry, University of Mysore, Manasagangotri, Mysore 570006, India; sindhump9164@gmail.com (S.M.P.); akshayrv533@gmail.com (A.R.); arunmysore3@gmail.com (A.M.); dukanya4@gmail.com (D.D.); preethamhd26@gmail.com (H.D.P.)
2 Shenzhen Bay Laboratory, Shenzhen 518055, China; zhangxi@szbl.ac.cn (Z.X.); pelobie@sz.tsinghua.edu.cn (P.E.L.)
3 Department of Chemistry, Central College Campus, Bangalore University, Bangalore 560001, India; svanishree00@gmail.com (V.S.); ganga.periyasamy@gmail.com (G.P.)
4 Department of Chemistry, BITS-Pilani Hyderabad Campus, Jawahar Nagar, Medchal, Hyderabad 500078, India; f20210833@hyderabad.bits-pilani.ac.in
5 Department of Chemistry, Manipal Institute of Technology, Manipal Academy of Higher Education, Manipal 576104, India; sl.gaonkar@manipal.edu
6 Tsinghua Berkeley Shenzhen Institute, Tsinghua Shenzhen International Graduate School, Tsinghua University, Shenzhen 518055, China
7 Institute of Biopharmaceutical and Health Engineering, Tsinghua Shenzhen International Graduate School, Tsinghua University, Shenzhen 518055, China
* Correspondence: vijay.pandey@sz.tsinghua.edu.cn (V.P.); basappa@chemistry.uni-mysore.ac.in or salundibasappa@gmail.com (B.B.)

check for updates

Citation: Parameshwaraiah, S.M.; Xi, Z.; Ravish, A.; Mohan, A.; Shankarnaik, V.; Dukanya, D.; Basappa, S.; Preetham, H.D.; Periyasamy, G.; Gaonkar, S.L.; et al. Development of an Environment-Friendly and Electrochemical Method for the Synthesis of an Oxadiazole Drug-Scaffold That Targets Poly(ADP-Ribose)Polymerase in Human Breast Cancer Cells. *Catalysts* **2023**, *13*, 1185. https://doi.org/10.3390/catal13081185

Academic Editor: Jose M. Guisan

Received: 28 June 2023
Revised: 22 July 2023
Accepted: 23 July 2023
Published: 4 August 2023

Abstract: The development of environment-friendly new Poly-adenosine diphosphate (ADP)-ribose Polymerase (PARP) inhibitors are highly essential because of their involvement in the survival of cancer cells. Therefore, a library of indazolyl-substituted-1,3,4-oxadiazoles known to inhibit PARP in cancer cells was synthesized by a green protocol. Furthermore, the cytotoxic effects of these compounds were evaluated in human MCF-7 breast cancer (BC) cells, which revealed that the compound 2-(3-bromo-4-nitrophenyl)-5-(1-methyl-1*H*-indazol-3-yl)-1,3,4-oxadiazole (**8**) inhibited viability with an IC_{50} value of 1.57 μM. Since the oxadiazole structure was extensively used in medicinal chemistry applications, the reported environment-friendly protocol was superior to the conventional method. Further, computational mechanistic studies revealed that the oxadiazole ring formation occurred spontaneously when compared to the conventional method. Additionally, the in silico bioinformatic studies of oxadiazole binding towards PARP1 showed that compound **8** could bind to PARP1 with higher binding energy (BE) of −7.29 kcal/mol when compound to compound 5s (BE = −7.17 kcal/mol), a known PARP cleavage oxadiazole structure (2-(3,4-Dimethoxybenzyl)-5-(3-(2-fluoro-3-methylpyridin-4-yl)phenyl)-1,3,4-oxadiazole) indicative of the improvement in the optimization process. In conclusion, a newer indazolyl-oxadiazole compound is reported, which could serve as a lead in developing PARP inhibitors in BC cells.

Keywords: 1,3,4-oxadiazoles; poly(ADP-ribose) polymerase; human breast cancer; auto dock; density function theory

1. Introduction

The "green approach" is a cutting-edge chemistry development that seeks to reduce or eliminate using hazardous compounds in chemical reactions [1]. Green chemistry plays an

essential role as it is safer, has high atom utilization, is economical, and is environmentally friendly [2,3]. Electrochemical synthesis is now becoming a widely used technique by chemists [3–5]. The reaction systems often do not need any additional activation since reactions happen by direct electron transfer at the electrode. Hence the conditions are moderate, and the selectivities are high [6].

In the design and synthesis of anti-cancer medicines, oxadiazoles are frequently used as critical building block units [7]. These scaffolds can be modified to maximize the compounds' intended biological activity, pharmacokinetics, and toxicity profile [8,9]. As a result, there is a growing interest in the field of drug discovery and design for oxadiazole-based drug scaffolds [10,11]. Approptiately, further oxadiazole-containing anti-cancer medications may have been identified or are currently being developed [12]. Biologically, oxadiazole derivatives target multiple signaling pathways that are involved in cancer progression [13,14]. In addition, oxadiazole compounds possess a range of biological impacts, such as inhibiting the polymerization of micro-tubulins, as well as anti-proliferative, and apoptosis-inducing features [15–17].

Furthermore, oxadiazole-based compounds were also designed as kinase inhibitors that are associated with cancer-signaling pathways [18]. These compounds can interfere with kinase activity and disrupt downstream signaling, which in turn induces the death of cancer cells [19–21]. Additionally, a few oxadiazole derivatives can intercalate into DNA, disrupting DNA replication and transcription processes and thereby inhibiting cancer cell proliferation, and promoting apoptosis in BC cells [22–24].

Olaparib, Rucaparib, and Niraparib are a few PARP inhibitors [25] that have been designed and approved for clinical use in the treatment of various malignancies, mainly ovarian and breast cancers [26,27]. As a crucial architectural motif, such chemicals often include an oxadiazole core that interacts with the active site of PARP enzymes to block their catalytic activity [28]. Through the inhibition of PARP enzymes, oxyadiazole-based PARP inhibitors restrict DNA repair in cancer cells, accumulating DNA damage [29]. This additional DNA damage eventually results in cancer cells dying [30,31].

Oxadiazole-based compounds were designed and synthesized as PARP inhibitors to take advantage of cancer cells with compromised DNA repair mechanisms, such as those with BRCA mutations [32]. Targeting PARP enzymes can result in synthetic lethality, in which cancer cells are selectively eradicated while normal cells are least affected [33].

Ditazole, an oxazole-based drug, inhibited the platelet aggregation either by inhibiting the ADP-reptilase clot retraction or also inhibited modified thrombin-induced clot formation [34]. Zibotentan (ZD4054) is an oxadiazole drug used for cancer treatment [35], and others like Furamizole, Raltegravir, and Nesapidil are among the drugs containing an oxadiazole motif [36]. Oxadiazoles are well known for their anti-cancer activity [37–40]. C1 bearing an oxadiazole moiety was observed to inhibit PARP1 activity with an IC_{50} as low as 1 nM, resulting in a cellular EC50 of 3.7 nM, combined with an excellent pharmacokinetic profile [41].

The tankyrase inhibitor G007-LK was discovered to co-crystallize with the TNKS2 PARP catalytic domain and bound to PARP's expanded adenosine binding pocket, demonstrating specific oxadiazole affinity to PARP catalytic domains [42].

Various heterocycles along with oxadiazoles have been shown to increase the anti-cancer efficacy of the oxadiazoles, such as pyrazole-substituted oxadiazoles [43], pyridine-based oxadiazoles [44], benzothiazole and piperazines substituted oxadiazoles [45], and benzotriazoles clubbed oxadiazoles [46]. Indole-added oxadiazoles (**L1**) were efficacious against MDA-MB-231, HeLa, and KGla cells, and further studies showed that the compound targets the BCL2 protein [47]. Quinolin-tethered oxadiazoles (**L2**) inhibited HepG2, SGC-7901, and MCF-7 cells by targeting telomerase enzyme [48].

Previously, we reported oxadiazole hybrids (**L3**, **L4**) as inhibitors of PARP [49,50]. The laboratory also reported the synthesis of indazole-substituted oxadiazole compounds and identified lead structures (**L5**) [51,52] and (**L6**) as PARP inhibitors, which decreased the viability of BC cells with an IC_{50} value of a 1.4 micromolar when compared to Olaparib (3.2 micromolar) [53].

The oxadiazole ring has a pivotal role in anti-cancer drug design and discovery, chemists employ various synthetic strategies to introduce the oxadiazole ring into drug candidates by using traditional organic synthesis, combinatorial chemistry, or electrochemical synthesis. Oxadiazole ring cyclization via electrochemical synthesis provides higher yields of the desired product and could be isolated and purified via the green chemical method [54,55]. However, the detailed comparison of the synthesis of oxadiazole ring using traditional over electrochemical methods and the determination of computational mechanism needs to be clarified. Therefore, in this report, we synthesized, characterized, and identified an improved route of synthesis (conventional over electrochemical) of oxadiazoles that targets PARP in human BC cells (**L7**, Figure 1). Furthermore, the computational analysis to model and simulate the reaction steps involved in the cyclization of oxadiazoles was performed, which provided insight into the energy profile of the reaction, transition states, reaction pathways, and intermediates [56].

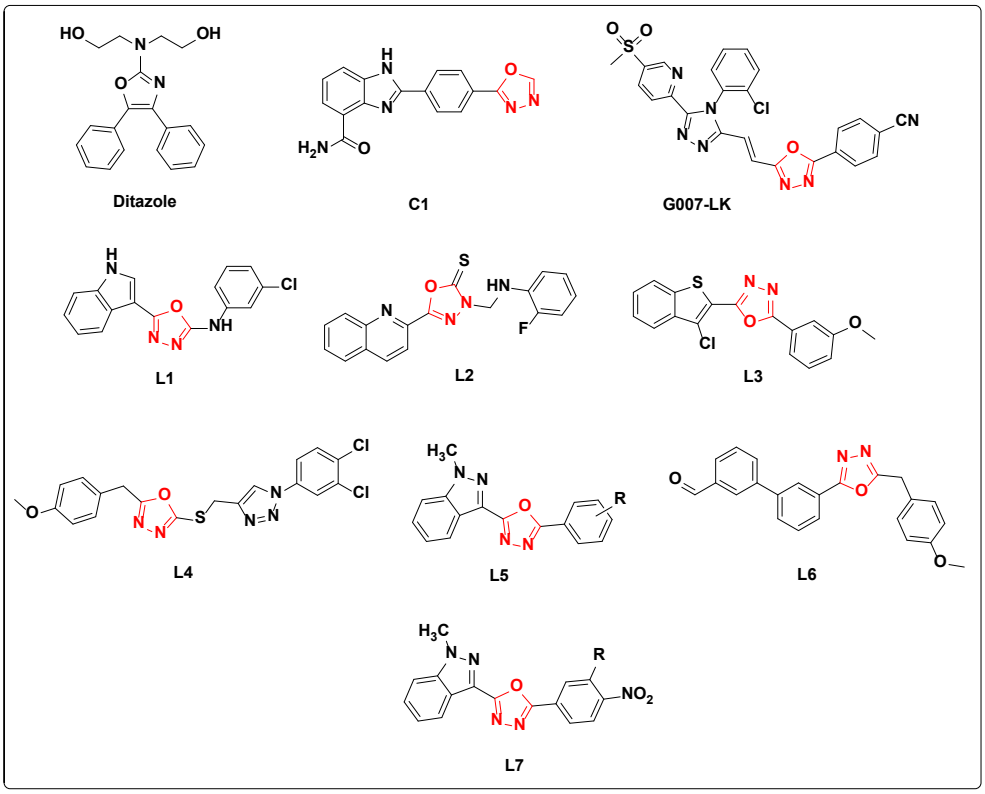

Figure 1. Evolution of oxadiazole (red)-based drugs/bioactive structures.

2. Results and Discussion

2.1. Chemical Synthesis of 1,3,4-Oxadiazoles via Conventional Methods

Indazole acid hydrazide (**1**) was synthesized by esterification followed by refluxing with hydrazine hydrate and further intermolecular cyclization with 3-bromo-4-nitrobenzoic acid using $POCl_3$ as a cyclizing agent yields 1,3,4 oxadiazole (**8**) (Schemes 1 and 2). Usually, $POCl_3$, $SOCl_2$, Conc. H_2SO_4, or tosyl chloride, mediates [57,58] the cyclodehydration processes. Oxadiazoles can be synthesized using a variety of methods. Still, most are environmentally harmful as they either directly or indirectly require highly toxic or corrosive chemicals, strong alkaline or acidic conditions, or emit thiol as an unwanted byproduct. The associated downsides include high temperature, protracted reaction periods, and hygroscopic chemicals. A more sustainable synthesis is crucial, especially considering the characteristics of 1,3,4-oxadiazoles.

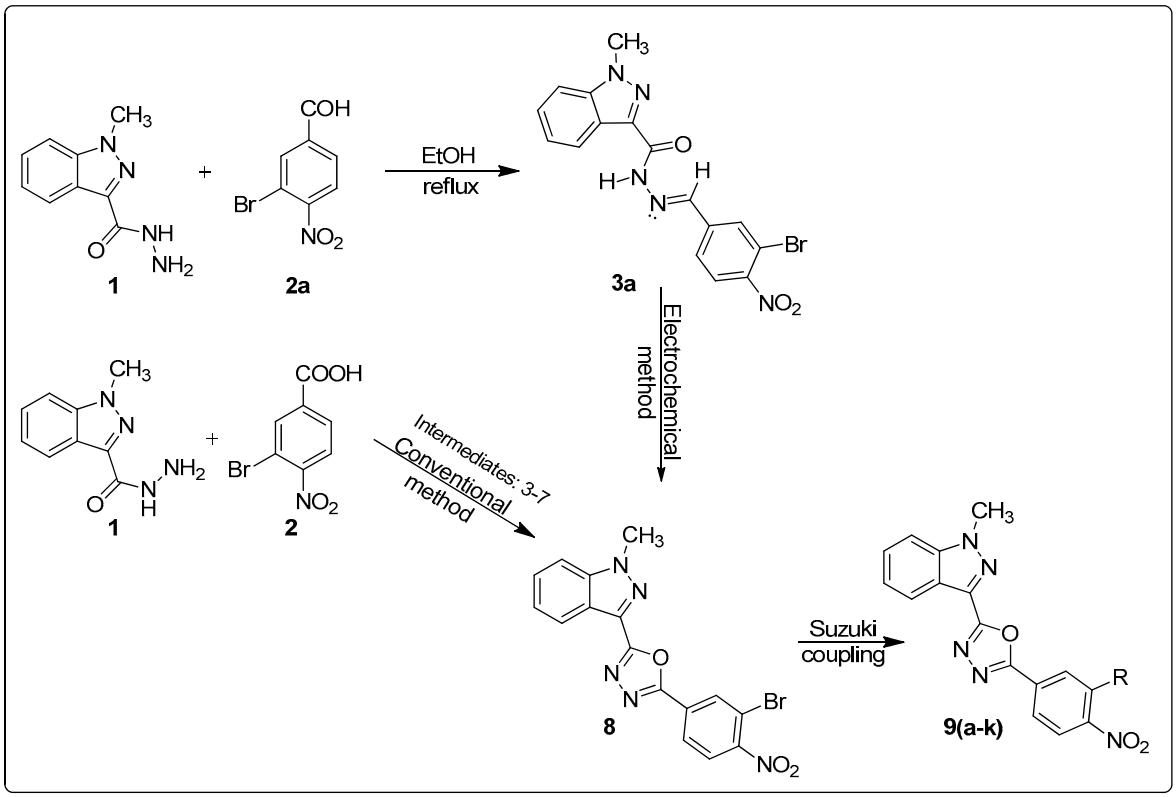

Scheme 1. Synthesis of novel substituted oxadiazoles **9a–k**.

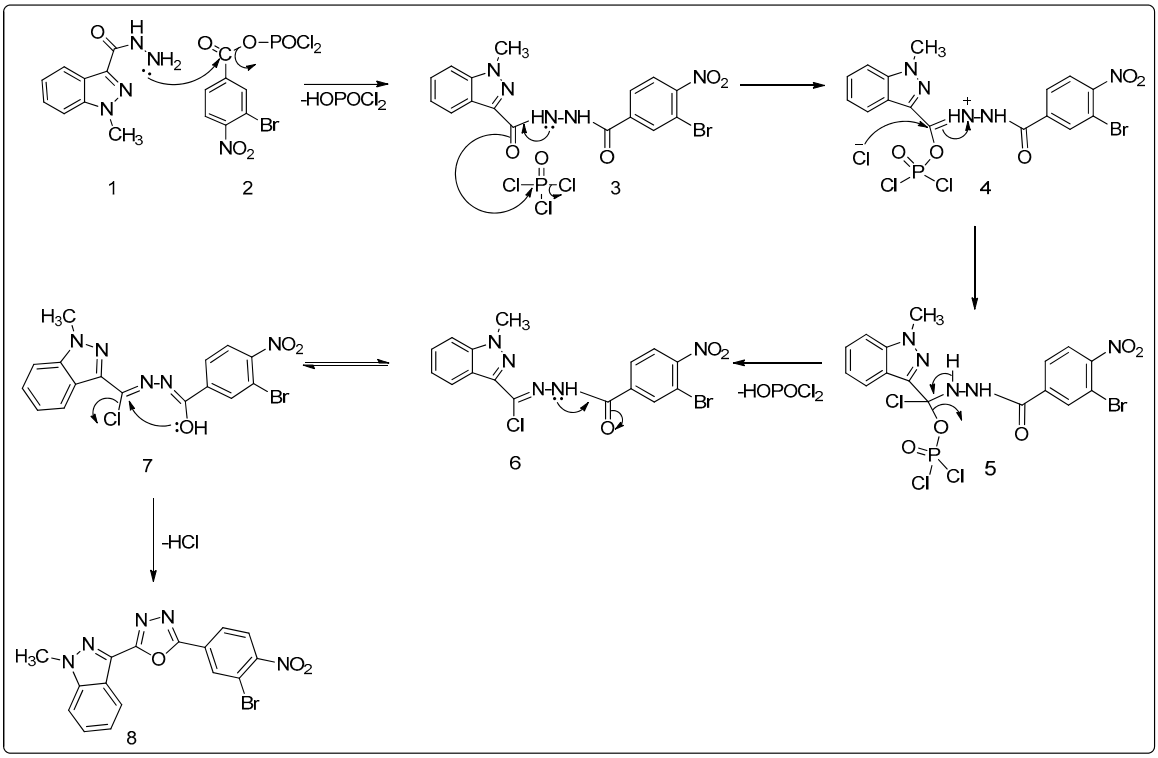

Scheme 2. The proposed mechanism via $POCl_3$-mediated cyclization.

The mechanism goes through the lone pair of electrons on the nitrogen atom of acid hydrazide, attacks the carbonyl carbon atom of carboxylic acid and eliminates a water molecule to form a hydrazide derivative. This hydrazide derivative then reacts with phosphorus oxychloride and undergoes ring closure with the elimination of hydrogen chloride, forming the 1,3,4-oxadiazole ring.

2.2. Synthesis of 1,3,4-Oxadiazoles via the Electrochemical Method

Using cyclic voltammetry and controlled potential electrolysis, the electrochemical oxidation of (E)-*N*′-(3-bromo-4-nitrobenzylidene)-1-methyl-1*H*-indazole-3-carbo-hydrazide using $NaClO_4$ as a supporting electrolyte in methanol has been investigated. The intramolecular cyclization occurs at the platinum electrode in an undivided cell with a yield of 85% of 1,3,4-oxadiazoles under room temperature. Indazole acid hydrazide (**1**) was treated with 3-bromo-4-nitrobenzaldehyde (**2a**) and yields hydrazone (**3a**) by two-electron oxidation followed by deprotonation and intermolecular cyclization yields oxadiazole (**8**) [59].

Further, (**8**) subjected to Suzuki coupling with various boronic acids (Table 1) to yield compounds (**9a**–**k**) (Schemes 1 and 3) (Table 2)**.**

Table 1. List of R groups and structure.

Boronic Acids (R)	Structure
Pyridin-3-Ylboronic Acid	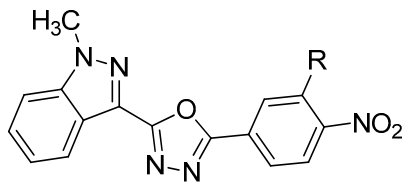
Pyridin-4-Ylboronic Acid	
(6-Chloro-5-Methylpyridin-3-Yl)Boronic Acid	
(2-Fluoro-3-Methylpyridin-4-Yl)Boronic Acid	
(4-Chlorophenyl)Boronic Acid	
Benzofuran-2-Ylboronic Acid	
Cyclopentylboronic Acid	
(3-(Cyclopentylcarbamoyl)Phenyl)Boronic Acid	
(4-Bromophenyl)Boronic Acid	
(4-Formylphenyl)Boronic Acid	
Phenylboronic Acid	

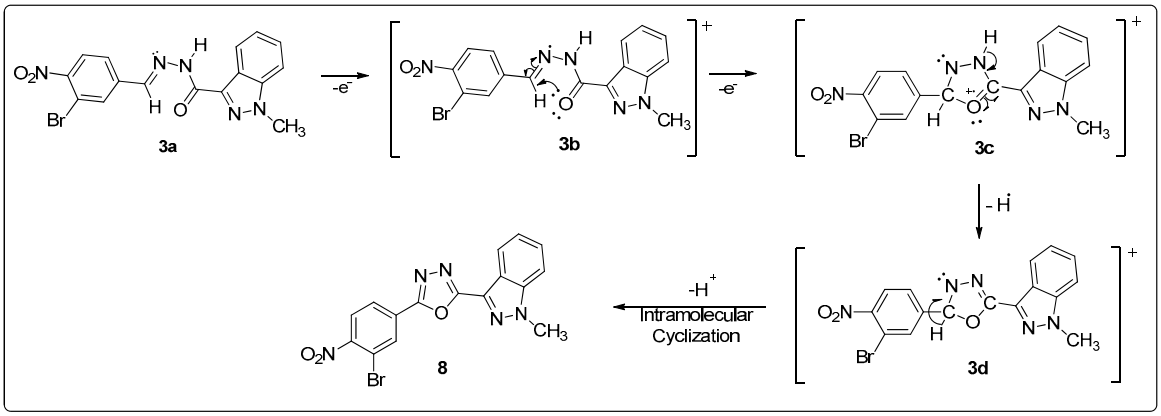

Scheme 3. The electrochemical synthesis of oxadiazoles **6**(**a**–**k**).

Table 2. Effect of newly synthesised compounds on viability of MCF-7 cells.

Compounds	IC_{50} (μM)	Compounds	IC_{50} (μM)
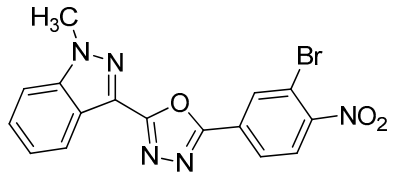 **8**	1.57	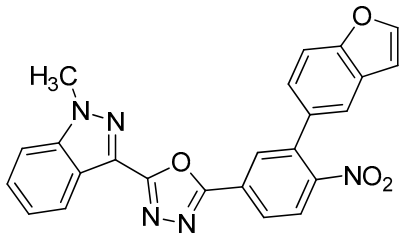 **9f**	84.70
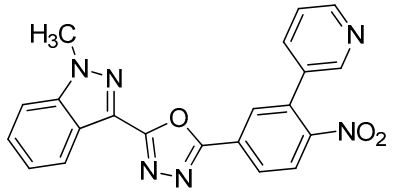 **9a**	36.36	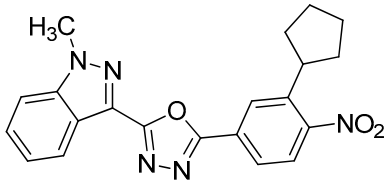 **9g**	>100
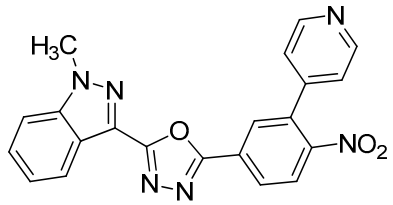 **9b**	>100	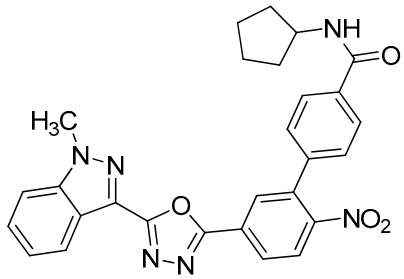 **9h**	51.23
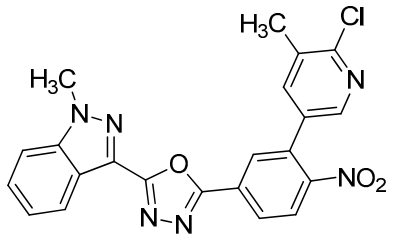 **9c**	62.07	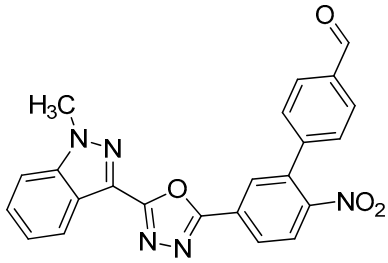 **9i**	76.84
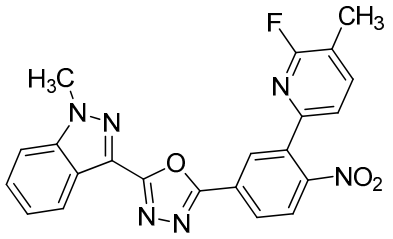 **9d**	>100	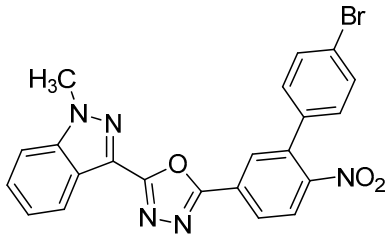 **9j**	46.85
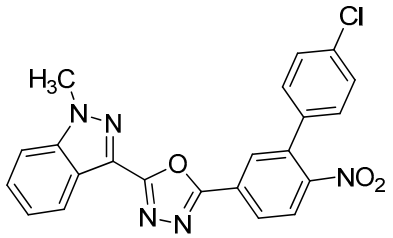 **9e**	64.89	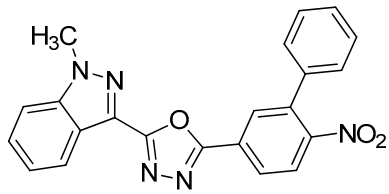 **9k**	44.40

2.3. DFT Calculations

Further, to study DFT calculations, all structures were optimized with CAM-B3LYP functional and 6-31+G(d) basis set for all atoms using the Gaussian 09 package. The normal mode analysis has been carried out to characterize the minima and saddle points. The presence of a single imaginary frequency corresponding to the bonds involved in the reaction is used to characterize the transition states. Further, the intrinsic reaction coordinate analyses have been performed in both forward and backward reactions to determine the transition state along the reaction pathway. The reaction follows TS1/TS1a, INT1, INT1A, TS2, INT2, INT3, INT4, INT5, and TS3 to reach the product (Figure 2). The reaction shows an exothermic nature, where we observed an energy release of 30 kcal mol^{-1}. The addition of reactants (**1**) and (**2**) takes place on or before the deprotonation of reactant (**1**). We computed both possibilities, leading to intermediates INT1 and INT1A (**3**) via TS1 and TS1A. This step is the rate-determining the largest energy barrier in the reaction energy profile.

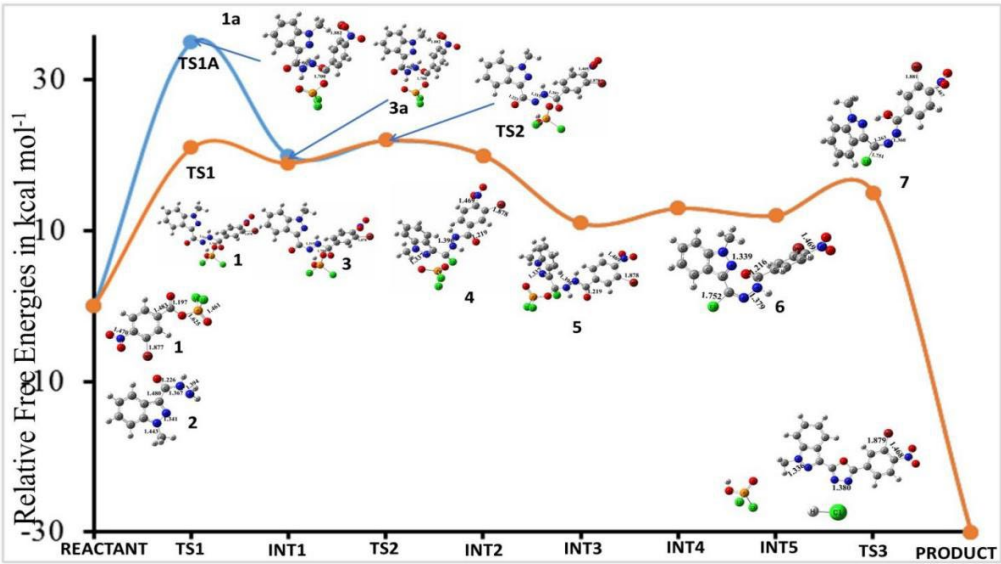

Figure 2. Computed reaction mechanism with relative energy profile. Energies are given in kcal mol^{-1} and the essential bond distances are shown.

The addition after deprotonation is more favorable via TS1 by 21 kcal mol^{-1}. INT1 undergoes rearrangement of Cl to form INT2. The lowest energy barrier of TS2 is due to the steric nature of two chlorines in the reactions. Then, INT2 undergoes the proton transfer and removal of $HOPOCl_2$, forming the stable states INT3, INT4, and INT5. The cyclization of INT5 leads to the product by removing the HCl molecule, which requires 12 kcal mol^{-1} energy via TS3.

Further, the optimization of (**3a**) shows the charge separation where HOMO and LUMO localize at the aromatic ring at the opposite end. Removing electrons from localized HOMO requires 7 eV energy that makes the carbonyl unit in (**3a**) charge deficient. The optimization of ionized species leads to (**3c**), which is highly energetic by 0.16 eV compared to (**3a**). The (**3c**) has highly active hydrogen. Removing a H+ ion leads to (**3c**), which has 0.19 eV higher in energy than (**3a**). The removal of one more -H+ ion leads to a stable product. The complete reaction is exothermic, where the product is more stable than the reactant by −0.844 eV energy (Figure 3).

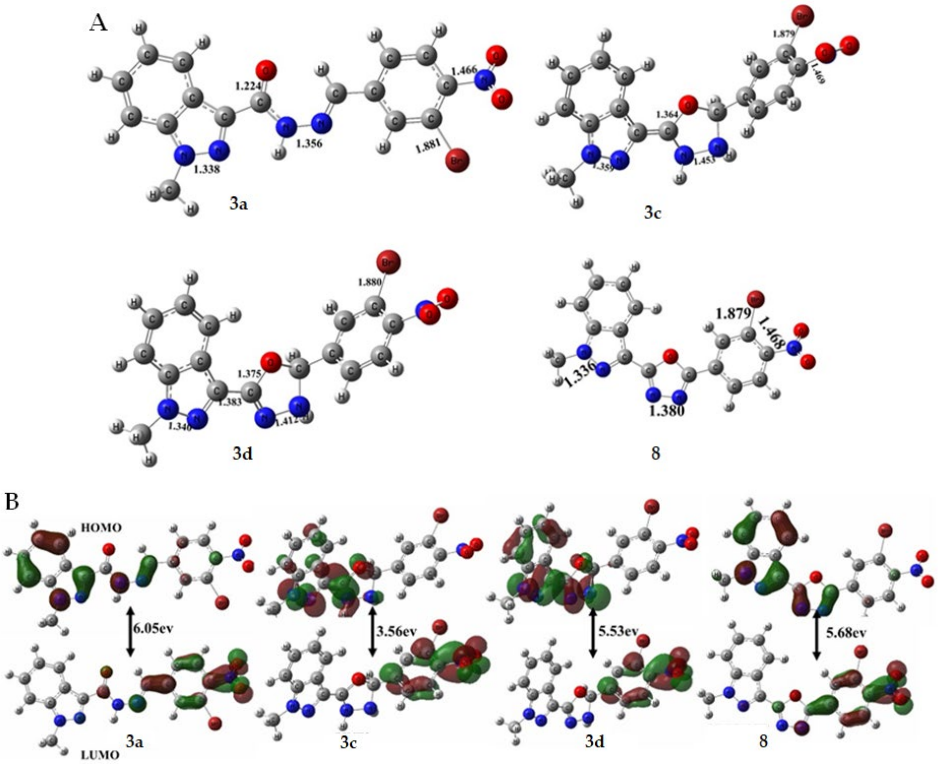

Figure 3. (**A**) Optimized structure of various possible states through electrolysis method. (**B**) Computed highest occupied (HOMO) and lowest unoccupied molecular orbital (LUMO) of stable states in the electrolysis method. The HOMO-LUMO gaps are given in eV.

2.4. Efficacy of Oxadiazoles in Breast Cancer Cells

The newly synthesized indazoyl-oxadiazoles (**9a**–**k**) were evaluated for loss of cell viability in human breast cancer (MCF-7) cells using Alamar Blue assays (Figure 4). Internal control, Tamoxifen, and Doxorubicin produced a loss of viability of MCF-7 cells with IC_{50} values of 1.79 and 0.71 μM, respectively. Compound (**8**) exhibited an IC_{50} of 1.57 μM, and the other 11 boronic acid derivatives showed IC_{50}s between 36.36 and 100.00 μM.

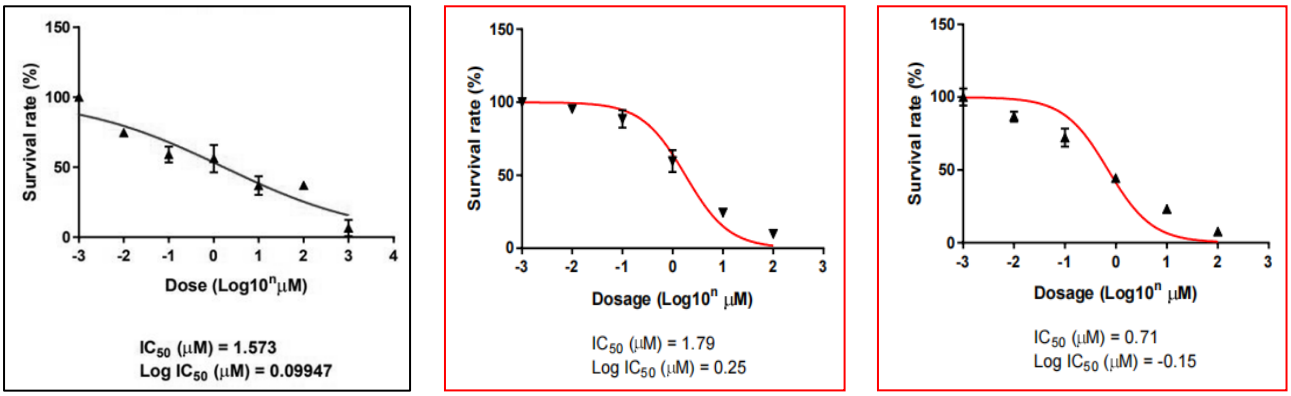

Figure 4. IC_{50} curves of lead compound **8** (black), Tamoxifen, and Doxorubicin (red) against MCF-7 BC cells using Alamar Blue assay.

*2.5. In Silico Analysis of the Interaction of Compound **8** with the PARP1 Catalytic Domain*

To understand the interaction of the novel oxadiazoles with the PARP1 catalytic domain, a bioinformatic analysis to understand the compound (**8**) 2-(3-bromo-4-nitrophenyl)-5-(1-methyl-1*H*-indazol-3-yl)-1,3,4-oxadiazole-binding affinity towards the PARP1 catalytic

domain was performed, using the reported crystal structure (PDB ID: 4HHY). AutoDock 4 version 1.5.6 was used for molecular docking. Active oxadiazole compound (**8**) was docked towards the PARP1 catalytic domain, which showed a binding affinity of −7.29 kcal/mol. The detailed molecular interactions between the amino acid residues of PARP1 catalytic domain and compound (**8**) are shown in Figures 5 and 6. The molecular interactions of compound (**8**) exhibited higher binding affinities with the PARP1 catalytic domain by having two hydrogen bonds with LYS-232 and LEU-280 with bond distances of 1.9 Å and 2.4 Å, respectively. The binding energies of all the docked molecules are given in (Table 3). As previously reported, compound **5s** [13] was found to be effective against both MCF-7 and MDA-MB-231 cells by inhibiting PARP1 activity that led to the increased cleavage of PARP1. The binding energy of compound **5s** was found to be −7.17 kcal/mol when docked towards the PARP1 catalytic domain (PDB ID:4HHY). The active compound (**8a**) was compared with the previously reported oxadiazole compound **5s,** which depicts that the active compound (**8a**) showed better binding energy (−7.29 kcal/mol) than compound **5s** (−7.17 kcal/mol), which is almost similar in range. The docking studies reveal that the active compound (**8**) targets the PARP1 active site, and decreases the viability of human breast cancer cells.

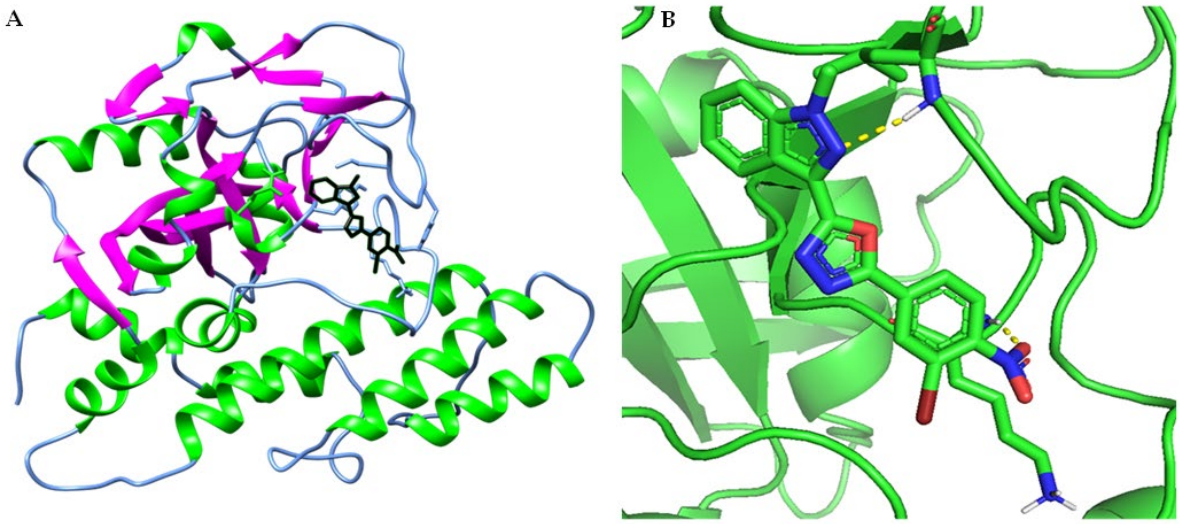

Figure 5. (**A**) Cartoon representation of docked compound (**8**) into PARP1 catalytic domain. (**B**) Showing hydrogen bond formation between compound (**8**) with amino acid residues of LYS-232 and LEU-280 and having the bond distance of 1.9 Å and 2.4 Å, respectively.

Table 3. Binding energy of oxadiazoles with PARP1.

Entry	Binding Energy (kcal/mol)	Entry	Binding Energy (kcal/mol)
8	−7.29	**9f**	−8.67
9a	−7.43	**9g**	−7.75
9b	−9.28	**9h**	−8.44
9c	−7.62	**9i**	−8.11
9d	−8	**9j**	−7.94
9e	−7.86	**9k**	−7.52

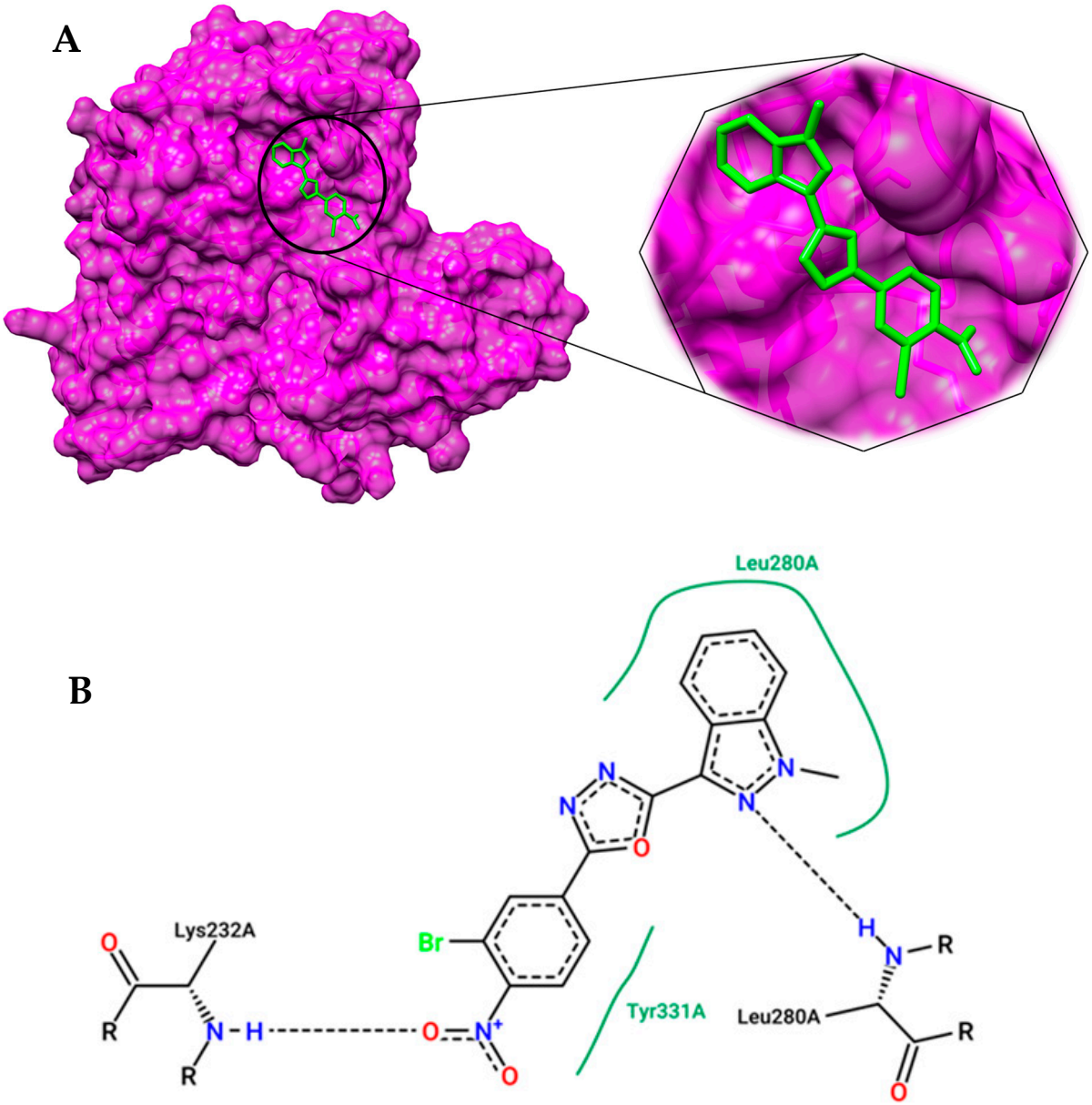

Figure 6. (**A**) 3D surface view of compound (**8**) with PARP1 and an enlarged view of compound, **8** (green) inside the active site of PARP1. (**B**) 2D structure of compound (**8**) showing interactions inside the binding pockets of PARP1.

3. Materials and Methods

All chemicals and solvents were purchased from Sigma-Aldrich (Bangalore, India). Analytical grade TLCs were used to monitor the reaction using ethyl acetate and hexane as eluent and observed under UV light. ^{1}H and ^{13}C NMR were recorded on an Agilent, NMR spectrophotometer (400 MHz; Agilent Technologies India Pvt. Ltd., Bangalore, India); TMS was used as an internal standard, and $CDCl_3$ and DMSO were used as solvents; chemical shifts were expressed as ppm downfield relative to the TMS. Mass spectra were recorded on Agilent LC-MS (Agilent Technologies India Pvt. Ltd., Bangalore, India). Column chromatography is used to purify compounds on silica gel (60–120 mesh).

3.1. General Procedure for Synthesizing New Oxadiazoles via the Conventional Method

The 1-methyl-1*H*-indazole-3-carboxylic acid (1 mmol) was refluxed with a catalytic amount of concentrated sulfuric acid in ethanol for 7 h. After completion of the reaction,

the reaction mass was cooled, and ethanol was removed by high vacuum pressure and neutralized by bicarbonate solution. The solid was filtered, and dried ethyl ester was obtained as a white solid. Ester (1 mmol) and hydrazine hydrate (1.2 mmol) were refluxed in ethanol for 5 h. After the completion of the reaction, the solid was filtered off, and the traces of hydrazine hydrate were washed with water. To a mixture of acid hydrazide (**1**) (1 mmol) and 3-bromo-4-nitrobenzoic acid (**2**) (1 mmol), 6 mL of $POCl_3$ was added and refluxed at 80 °C for 8 h. After completion of the reaction, the reaction mass was quenched with crushed ice and neutralized by K_2CO_3. The solid obtained was filtered, washed with water, and purified by column chromatography (hexane/ethyl acetate eluents) to obtain pure oxadiazole (**8**). Oxadiazole (**8**) (1 mmol), substituted boronic acids (1.2 mmol), and catalyst (Pd (dppf) Cl_2) (0.1 mmol) were added, and K_2CO_3 (3 mmol) was taken in a sealed tube containing the H_2O:THF (1:4) solvent and heated to 120 °C for 4–5 h. After the completion of the reaction, the crude reaction mass was extracted with ethyl acetate–water, and the combined organic layer was concentrated at reduced pressure. The obtained product was purified using hexane/ethyl acetate using a chromatographic technique. The molecules complete characterization data were provided as a supplementary data.

3.2. General Procedure for Synthesizing New Oxadiazoles via the Electrochemical Method

Acid hydrazide (**1**) (1 mmol) and 3-bromo-4-nitrobenzaldehyde (**2**) were refluxed in ethanol for 6 h. After completion of the reaction, the reaction mass was cooled, and ethanol was removed using high vacuum pressure. The crude was purified through column chromatography, yielding a compound (**3a**).

In a 250 mL three-neck round bottom flask electrode cell assembly with platinum plates as the working electrode, counter electrode, and reference electrode, electrolysis was carried out at room temperature. An undivided cell with a magnetic stirrer was used to perform controlled potential electrolysis (CPE) to a solution of a substrate (**3a**) (10 mmol) in dry MeOH (80 mL) that also contained $NaClO_4$ (5 mmol) as a supporting electrolyte. The reference electrode was kept close to the working electrode to reduce the ohmic drop. The electrolysis process was monitored by periodically noting the current drops over time. When the reaction was completed, as monitored by TLC, the cell was removed from the circuit, and the solvent was evaporated in a vacuum. Dry diethyl ether and water (1:1) were stirred over the residue to remove the supporting electrolyte. The resulting residue was purified with EtOH. By comparing the results of their LCMS, ^{1}H NMR, and ^{13}C NMR spectroscopy, the structures of the products (**8**) were confirmed.

*3.3. The 2-(3-bromo-4-nitrophenyl)-5-(1-methyl-1H-indazol-3-yl)-1,3,4-oxadiazole (**8**)*

Yellow solid; MP: 170–172 °C; NMR (400 MHz, $CDCl_3$) δ 8.55 (d, *J* = 1.6 Hz), 8.35 (d, *J* = 8.4 Hz), 8.26 (dd, *J* = 8.4, 1.6 Hz), 7.94 (d, *J* = 8.4 Hz), 7.53–7.43 (m), 7.39–7.34 (m), 4.19 (s); mass spectra; calculated for $C_{16}H_{10}BrN_5O_3$ 400.19, found 322.0042 $[M\text{-}Br]^+$.

*3.4. The 2-(1-methyl-1H-indazol-3-yl)-5-(4-nitro-3-(pyridin-3-yl)phenyl)-1,3,4-oxadiazole (**9a**)*

Brown solid; MP: 160–163° C; 88% yield; ^{1}H NMR(400 MHz) δ 8.71 (s, 1H), 8.38 (s, 1H), 8.42–8.38 (m, 2H), 8.13 (d, *J* = 6 Hz, 1H), 7.71 (d, *J* = 6 Hz, 1H), 7.54–7.43 (m, 2H), 7.43–7.39 (m, 2H), 4.22 (s, 3H); ^{13}C NMR (100 MHz) δ 161.92, 161.16, 159.66, 150.20, 149.91, 148.45, 141.08, 141.01, 135.59, 134.24, 132.62, 130.52, 128.91, 127.83, 127.75, 127.59, 127.36, 125.56, 123.42, 122.96, 122.47, 122.07, 121.92, 109.65, 109.46, 36.47, 36.33; mass spectra; calculated for $C_{21}H_{14}N_6O_3$ 398.3743, found 399.2017 $[M+1]^+$.

*3.5. The 2-(1-methyl-1H-indazol-3-yl)-5-(4-nitro-3-(pyridin-4-yl)phenyl)-1,3,4-oxadiazole (**9b**)*

Yellow solid; MP: 160–165 °C; 90% yield; ^{1}H NMR: (400 MHz) δ 8.75 (d, 2H), 8.28 (s, 1H), 8.47–8.41 (m, 2H), 8.15 (d, *J* = 8 Hz, 1H), 7.57–7.51 (m, 2H), 7.43–7.40 (m, 1H), 7.34–7.33 (m, 2H), 4.23 (s, 3H); ^{13}C NMR (100 MHz) δ 161.84, 161.18, 150.14, 149.77, 144.66, 141.08, 141.00, 135.10, 129.93, 129.33, 128.88, 127.94, 127.89, 127.78, 127.37, 125.56, 123.46, 122.96, 122.76, 122.47, 122.43, 122.08, 121.93, 109.66, 109.45, and 36.48.

*3.6. The 2-(3-(6-chloro-5-methylpyridin-3-yl)-4-nitrophenyl)-5-(1-methyl-1H-indazol-3-yl)-1,3,4-oxadiazole (**9c**)*

Off-white solid; MP: 180–182 °C; 85% yield; ^{1}H NMR; (400 MHz, $CDCl_3$) δ 8.45–8.41 (m, 2H), 8.28 (m, 2H), 8.16 (d, *J* = 12 Hz, 1H), 7.60–7.59 (m, 1H), 7.56–7.54 (m, 2H), 7.44–7.40 (m, 1H), 4.24 (s, 3H), 2.47 (s, 1H).^{13}C NMR (100 MHz) δ 161.85, 161.21, 152.19, 150.06, 145.55, 141.11, 138.73, 133.19, 132.66, 131.66, 130.46, 128.92, 127.94, 127.78, 125.66, 123.47, 122.50, 121.95, 109.66, 36.49, and 19.71.

*3.7. The 2-(3-(6-fluoro-5-methylpyridin-2-yl)-4-nitrophenyl)-5-(1-methyl-1H-indazol-3-yl)-1,3,4-oxadiazole (**9d**)*

Yellow solid; MP: 190–194 °C; 86% yield; ^{1}H NMR (400 MHz, $CDCl_3$) δ 8.43 (d, *J* = 4 Hz, 1H), 8.41 (d, *J* = 4 Hz, 1H), 8.28 (s, 1H), 8.14 (d, *J* = 8 Hz, 1H), 8.09 (d, *J* = 8 Hz, 1H), 7.65–7.63 (m, 1H), 7.58–7.52 (m, 2H), 7.46–7.40 (m, 1H), 4.24 (s, 3H), 2.38 (s, 3H).^{13}C NMR (100 MHz) δ 163.21, 161.90, 161.61,161.19, 150.23, 143.64, 143.54, 141.28, 141.11, 133.27, 130.56, 130.51, 130.48, 129.50, 128.90, 127.80, 127.64, 125.57, 123.48, 122.49, 121.93, 120.14, 119.92, 109.67, 36.49, and 14.56.

*3.8. The 2-(4′-chloro-6-nitro-[1,1′-biphenyl]-3-yl)-5-(1-methyl-1H-indazol-3-yl)-1,3,4-oxadiazole (**9e**)*

Yellow solid; MP:162–165 °C; 82% yield; ^{1}H NMR(400 MHz, $CDCl_3$) δ 8.41 (d, *J* = 8 Hz, 1H), 8.38–8.35 (m, 1H), 8.28 (d, *J* = 1H), 7.74 (s, 1H), 7.57–7.51 (m, 3H), 7.48–7.45 (m, 2H), 7.34–7.32 (m, 2H), 4.24 (s, 3H).^{13}C NMR (100 MHz) δ 162.09, 161.06, 150.42, 141.06, 136.31, 135.16, 134.62, 130.28, 129.32, 129.15, 127.77, 127.37, 127.03, 126.28, 125.16, 123.44, 122.43, 121.90, 116.68, 115.49, 109.65, and 36.46; mass spectra; calculated for $C_{22}H_{14}ClN_5O_3$ 431.8313, found 432.0977 $[M+1]^+$.

*3.9. The 2-(3-(benzofuran-6-yl)-4-nitrophenyl)-5-(1-methyl-1H-indazol-3-yl)-1,3,4-oxadiazole (**9f**)*

Brown solid; MP:173–175 °C; 89% yield; ^{1}H NMR (400 MHz, $CDCl_3$) δ 8.62 (d, 1H), 8.43–8.41 (m, 1H), 8.33–8.30 (m, 2H), 8.24–8.21 (m, 1H),8.00–7.98 (m, 1H), 7.56–7.54 (m, 2H), 7.46 (d, 2H), 7.34–7.30 (m, 2H), 4.25 (s, 3H). ^{13}C NMR (100 MHz) δ 162.70, 161.16, 151.16, 141.08, 141.03, 133.27, 129.32, 128.83, 128.23, 127.80, 126.91, 126.68, 126.30, 123.67, 123.48, 123.10, 122.48, 122.25, 121.93, 120.72, 115.50, 109.67, 109.49, and 61.03.

*3.10. The 2-(3-cyclopentyl-4-nitrophenyl)-5-(1-methyl-1H-indazol-3-yl)-1,3,4-oxadiazole (**9g**)*

Off-white solid; MP:190–195 °C; 80% yield; ^{1}H NMR(600 MHz) δ 8.65 (d, *J* = 4 Hz, 1H), 8.41–8.39 (m, 1H), 8.32–8.30 (m, 1H), 7.99 (d, *J* = 8 Hz, 1H), 7.56–7.51 (m, 2H), 7.43–7.40 (m, 1H), 4.24 (s, 3H), 1.42–1.40 (m, 1H), 1.25–1.24 (m, 2H). ^{13}C NMR (151 MHz) δ 161.25, 161.16, 151.20, 141.11, 133.28, 129.50, 128.86, 128.27, 127.78, 126.69, 126.29, 123.48, 121.94, 115.50, 109.66, 38.93, 36.49, 31.94, 31.63, 29.71, and 29.37.

*3.11. The N-cyclopentyl-5′-(5-(1-methyl-1H-indazol-3-yl)-1,3,4-oxadiazol-2-yl)-2′-nitro-[1,1′-biphenyl]-4-carboxamide (**9h**)*

Yellow solid; MP:192–195 °C; 78% yield; ^{1}H NMR (400 MHz, $CDCl_3$) δ 8.00 (d, J = 8 Hz, 1H), 8.06(d, *J* = 8 Hz, 1H), 8.42–8.30 (m, 6H), 8.61 (s, 1H), 7.87–7.80(m, 3H), 4.48–4.41 (m, 1H), 4.23 (s, 3H), 2.16–2.04 (m, 4H) 1.58–1.47 (m, 4H). ^{13}C NMR (100 MHz) δ 166.52, 162.06, 161.06, 151.14, 150.31, 141.05, 136.72, 135.74, 133.26, 130.70, 130.42, 129.04, 128.23, 127.34, 127.12, 126.52, 126.29, 125.19, 123.47, 123.41, 118.64, 109.64, 51.91, 51.75, 36.47, 33.20, 29.70, and 23.85.

*3.12. The 2-(4′-bromo-6-nitro-[1,1′-biphenyl]-3-yl)-5-(1-methyl-1H-indazol-3-yl)-1,3,4-oxadiazole (**9i**)*

Off-white solid; MP: 160–163 °C; 75% yield; ^{1}H NMR (600 MHz) δ 8.33 (d, *J* = 6 Hz, 1H), 8.30–8.29 (d, *J* = 6 Hz, 1H), 8.26 (d, *J* = 6 Hz, 1H), 8.03 (s, 1H), 7.98 (d, *J* = 12 Hz, 1H), 7.61–7.60 (m, 1H), 7.54–7.52 (m, 3H), 7.45–7.44 (m, 1H), 7.42–7.39 (m, 1H), 4.22 (s, 3H). ^{13}C NMR (100 MHz) δ 161.98, 150.26, 140.97, 136.24, 135.43, 135.01, 133.15, 131.99, 130.92, 130.12, 129.48, 127.67, 127.26, 126.95, 126.56, 126.16, 125.07, 123.35, 122.33, 121.76, 109.55, and 36.35.

*3.13. The 5′-(5-(1-methyl-1H-indazol-3-yl)-1,3,4-oxadiazol-2-yl)-2′-nitro-[1,1′-biphenyl]-4-carbaldehyde (**9j**)*

Brown solid; MP: 190–195 °C; 84% yield; ^{1}H NMR (400 MHz, $CDCl_3$) δ 8.62 (d, 1H), 8.43–8.41 (m, 1H), 8.34–8.31 (m, 1H), 8.24–8.21 (m, 1H), 8.00 (d, *J* = 8 Hz, 1H), 7.58–7.54 (m, 2H), 7.47–7.42 (m, 3H), 7.34–7.29 (m, 2H), 4.26 (s, 3H). ^{13}C NMR (100 MHz) δ 161.25, 161.16, 151.18, 141.09, 133.29, 133.27, 128.84, 128.26, 127.79, 126.90, 126.69, 126.30, 123.69, 123.48, 123.09, 122.49, 122.26, 121.93, 118.23, 115.50, 109.67, 109.50, and 36.50.

*3.14. The 2-(1-methyl-1H-indazol-3-yl)-5-(6-nitro-[1,1′-biphenyl]-3-yl)-1,3,4-oxadiazole (**9k**)*

Yellow solid; MP: 180–185 °C; 82% yield; ^{1}H NMR (400 MHz, $CDCl_3$) δ 8.42 (d, *J* = 8 Hz, 2H), 8.33 (d, *J* = 4 Hz, 2H), 8.24 (d, *J* = 8 Hz, 2H), 8.01 (s, 1H, br), 7.48–7.46 (m, 5H), 4.18 (s, 3H).^{13}C NMR (100 MHz) δ 162.27, 161.23, 150.68, 141.05, 135.63, 133.62, 132.69, 131.11, 130.50, 128.90, 127.98, 127.75, 127.15, 126.71, 126.30, 124.98, 123.42, 122.42, 121.92, 115.51, 109.64, and 36.46.

3.15. Cell Viability Assay

MCF-7 (2000) cells were cultured in MEM or Leibovitz's L-15 medium enriched with 2% FBS in a humidified atmosphere of 5% CO_2 at 37 °C [60]. Compounds were dissolved, kept as a stock solution, and diluted with a cell culture medium to the desired concentration. Cancer cells (4000) were grown in 96-well plates overnight, cultured, and treated with oxadiazoles at 0, 0.01, 0.1, 10, 100, and 1000 μM concentrations for 72 h. The inhibitory effect of the compounds was assessed using the Alamar Blue reagent. All the compounds IC50 curves were provided in the supplementary data.

*3.16. Bioinformatic Studies for the Compound (**8**)*

Bioinformatic analysis for the compound (**8**) was determined by using the Scripps Research Institute's AutoDock 4 [61] Tools (ADT) (v1.5.6). Furthermore, it was used to generate grid and docking parameter files. The crystal structure of PARP1 with a ligand was retrieved from the Protein Data Bank (PDB, accessed on 5 February 2023) [https://www.rcbs.org] using (PDB ID: 4HHY) and was then used for docking purposes. Further protein and ligand (compound **8**) preparations were done through the Discovery Studio Visualizer, and later it was used for docking in ADT (v 1.5.6) with the centroid rendered from the inhibitor in the crystallographic structure, the grid box size of 60 Å × 60 Å × 60 Å with 1 Å spacing is defined [62–66]. Also, as previously reported, compound 5 s was docked towards the PARP1 catalytic domain with a grid box size of 60 Å × 60 Å × 60 Å with 1 Å spacing. The empirical free-energy function and the Lamarckian genetic algorithm were used to perform molecular docking with the macromolecule with an initial population of 150 randomly placed individuals, a maximum number of 2,500,000 energy evaluations, a mutation rate of 0.02, a crossover rate of 0.80, and 10 docking runs were performed for compound 4. Visualization plots were examined using the BIOVIA Discovery Studio Visualizer (v21.1.0.20298) [67], pymol [68], and UCSF chimera 1.16 [69].

3.17. DFT Calculations

All the structures were optimized with CAM-B3LYP functional and 6-31+G(d) basis set for all atoms using the Gaussian 09 package. The standard mode analysis has been carried out to characterize the minima and saddle points [70].

4. Conclusions

In summary, we designed and synthesized novel indazoyl-substituted 1,3,4-oxadizoles as PARP1 inhibitors via conventional and electrochemical methods. DFT-Calculations evaluated the two methods. All the compounds were evaluated for their efficacy MCF-7 cells. The lead compound (**8**) exhibited an IC_{50} of 1.57 μM. Detailed in silico analysis showed that compound (**8**) could target PARP1 in MCF-7 cells.

Supplementary Materials: The following supporting information can be downloaded at https://www.mdpi.com/article/10.3390/catal13081185/s1. Supplementary data contain newly synthesized compounds NMR, LCMS, and IC_{50} values.

Author Contributions: S.M.P., Z.X., A.R., A.M., V.S., S.B. and D.D. conceptualization, methodology, formal analysis, and writing; S.L.G., H.D.P. and G.P., formal analysis, and writing; P.E.L., V.P. and B.B., conceptualization, methodology, software, data curation, original draft, validation, writing, and editing. All authors have read and agreed to the published version of the manuscript.

Funding: This work was supported by Vision Group on Science and Technology (CESEM) and the Government of Karnataka. This work was also supported by the Shenzhen Key Laboratory of Innovative Oncotherapeutics (ZDSYS20200820165400003) (Shenzhen Science and Technology Innovation Commission), China; the Shenzhen Development and Reform Commission Subject Construction Project ([2017]1434), China; the Overseas Research Cooperation Project (HW2020008) (Tsinghua Shenzhen International Graduate School), China; the Tsinghua University Stable Funding Key Project (WDZC20200821150704001); the Shenzhen Bay Laboratory (21310031), China; and TBSI Faculty Start-up Funds, China. Thanks to KSTePS (DST Ph.D. Fellowship), Karnataka, for funding A.R.

Data Availability Statement: All data are freely available within this article.

Conflicts of Interest: The authors declare no conflict of interest.

References

1. Yuan, Y.; Lei, A. Is Electrosynthesis always Green and Advantageous Compared to Traditional Methods? *Nat. Commun.* **2020**, *11*, 802. [CrossRef] [PubMed]
2. Jutand, A. Contribution of Electrochemistry to Organometallic Catalysis. *Chem. Rev.* **2008**, *108*, 2300–2347. [CrossRef] [PubMed]
3. Handler, G. Preface. *Commun. Asteroseismol.* **2007**, *150*, 10. [CrossRef]
4. Chen, Q.; Wang, X.; Tan, H.; Shi, W.; Zhang, X.; Wei, S.; Giesy, J.P.; Yu, H. Molecular Initiating Events of Bisphenols on Androgen Receptor-Mediated Pathways Provide Guidelines for In Silico Screening and Design of Substitute Compounds. *Environ. Sci. Technol. Lett.* **2019**, *6*, 205–210. [CrossRef]
5. Ganesh, K.N.; Zhang, D.; Miller, S.J.; Rossen, K.; Chirik, P.J.; Kozlowski, M.C.; Zimmerman, J.B.; Brooks, B.W.; Savage, P.E.; Allen, D.T.; et al. Green Chemistry: A Framework for a Sustainable Future. *Org. Process Res. Dev.* **2021**, *25*, 1455–1459. [CrossRef]
6. Anastas, P.; Eghbali, N. Green Chemistry: Principles and Practice. *Chem. Soc. Rev.* **2010**, *39*, 301–312. [CrossRef]
7. Jiang, Y.; Xu, K.; Zeng, C. Use of Electrochemistry in the Synthesis of Heterocyclic Structures. *Chem. Rev.* **2017**, *118*, 4485–4540. [CrossRef]
8. Ibrar, A.; Khan, A.; Ali, M.; Sarwar, R.; Mehsud, S.; Farooq, U.; Halimi, S.M.A.; Khan, I.; Al-Harrasi, A. Combined In Vitro and In Silico Studies for the Anticholinesterase Activity and Pharmacokinetics of Coumarinyl Thiazoles and Oxadiazoles. *Front. Chem.* **2018**, *6*, 61. [CrossRef]
9. Wang, S.; Qi, L.; Liu, H.; Lei, K.; Wang, X.; Liu, R. Synthesis of 1,3,4-Oxadiazoles Derivatives with Antidepressant Activity and Their Binding to the 5-HT1A Receptor. *RSC Adv.* **2020**, *10*, 30848–30857. [CrossRef]
10. Vaidya, A.; Pathak, D.; Shah, K. 1,3,4-oxadiazole and Its Derivatives: A Review on Recent Progress in Anticancer Activities. *Chem. Biol. Drug Des.* **2020**, *97*, 572–591. [CrossRef]
11. De Oliveira, C.S.; Lira, B.F.; Barbosa-Filho, J.M.; Lorenzo, J.G.F.; de Athayde-Filho, P.F. Synthetic Approaches and Pharmacological Activity of 1,3,4-Oxadiazoles: A Review of the Literature from 2000–2012. *Molecules* **2012**, *17*, 10192–10231. [CrossRef]
12. Biernacki, K.; Daśko, M.; Ciupak, O.; Kubiński, K.; Rachon, J.; Demkowicz, S. Novel 1,2,4-Oxadiazole Derivatives in Drug Discovery. *Pharmaceuticals* **2020**, *13*, 111. [CrossRef]
13. Rana, K.; Salahuddin; Sahu, J.K. Significance of 1,3,4-Oxadiazole Containing Compounds in New Drug Development. *Curr. Drug Res. Rev.* **2021**, *13*, 90–100. [CrossRef]
14. Taher, A.T.; Georgey, H.H.; El-Subbagh, H.I. Novel 1,3,4-Heterodiazole Analogues: Synthesis and In-Vitro Antitumor Activity. *Eur. J. Med. Chem.* **2012**, *47*, 445–451. [CrossRef]
15. Gu, W.; Jin, X.-Y.; Li, D.-D.; Wang, S.-F.; Tao, X.-B.; Chen, H. Design, Synthesis and In Vitro Anticancer Activity of Novel Quinoline and Oxadiazole Derivatives of Ursolic Acid. *Bioorganic Med. Chem. Lett.* **2017**, *27*, 4128–4132. [CrossRef]
16. Castanet, A.-S.; Nafie, M.S.; Said, S.A.; Arafa, R.K. Discovery of PIM-1 Kinase Inhibitors Based on the 2,5-Disubstituted 1,3,4-Oxadiazole Scaffold against Prostate Cancer: Design, Synthesis, In Vitro and In Vivo Cytotoxicity Investigation. *Eur. J. Med. Chem.* **2023**, *250*, 115220. [CrossRef]
17. Nieddu, V.; Pinna, G.; Marchesi, I.; Sanna, L.; Asproni, B.; Pinna, G.A.; Bagella, L.; Murineddu, G. Synthesis and Antineoplastic Evaluation of Novel Unsymmetrical 1,3,4-Oxadiazoles. *J. Med. Chem.* **2016**, *59*, 10451–10469. [CrossRef]
18. Basappa; Sugahara, K.; Thimmaiah, K.N.; Bid, H.K.; Houghton, P.J.; Rangappa, K.S. Anti-tumor activity of a novel HS-mimetic-vascular endothelial growth factor binding small molecule. *PLoS One* **2012**, *7*, e39444. [CrossRef]
19. Zoroddu, S.; Corona, P.; Sanna, L.; Borghi, F.; Bordoni, V.; Asproni, B.; Pinna, G.A.; Bagella, L.; Murineddu, G. Novel 1,3,4-Oxadiazole Chalcogen Analogues: Synthesis and Cytotoxic Activity. *Eur. J. Med. Chem.* **2022**, *238*, 114440. [CrossRef]

20. Glomb, T.; Świątek, P. Antimicrobial Activity of 1,3,4-Oxadiazole Derivatives. *Int. J. Mol. Sci.* **2021**, *22*, 6979. [CrossRef]
21. Yu, G.; Chen, S.; Guo, S.; Xu, B.; Wu, J. Trifluoromethylpyridine 1,3,4-Oxadiazole Derivatives: Emerging Scaffolds as Bacterial Agents. *ACS Omega* **2021**, *6*, 31093–31098. [CrossRef] [PubMed]
22. Jian, W.; He, D.; Song, S. Synthesis, Biological Evaluation and Molecular Modeling Studies of New Oxadiazole-Stilbene Hybrids against Phytopathogenic Fungi. *Sci. Rep.* **2016**, *6*, 31045. [CrossRef] [PubMed]
23. Szydłowski, M.; Prochorec-Sobieszek, M.; Szumera-Ciećkiewicz, A.; Derezińska, E.; Hoser, G.; Wasilewska, D.; Szymańska-Giemza, O.; Jabłońska, E.; Białopiotrowicz, E.; Sewastianik, T.; et al. Expression of PIM Kinases in Reed-Sternberg Cells Fosters Immune Privilege and Tumor Cell Survival in Hodgkin Lymphoma. *Blood* **2017**, *130*, 1418–1429. [CrossRef]
24. Szydłowski, M.; Dębek, S.; Prochorec-Sobieszek, M.; Szołkowska, M.; Tomirotti, A.M.; Juszczyński, P.; Szumera-Ciećkiewicz, A. PIM Kinases Promote Survival and Immune Escape in Primary Mediastinal Large B-Cell Lymphoma through Modulation of JAK-STAT and NF-κB Activity. *Am. J. Pathol.* **2021**, *191*, 567–574. [CrossRef] [PubMed]
25. Mohan, C.D.; Anilkumar, N.C.; Rangappa, S.; Shanmugam, M.K.; Mishra, S.; Chinnathambi, A.; Alharbi, S.A.; Bhattacharjee, A.; Sethi, G.; Kumar, A.P.; et al. Novel 1,3,4-Oxadiazole Induces Anticancer Activity by Targeting NF-κB in Hepatocellular Carcinoma Cells. *Front. Oncol.* **2018**, *8*, 42. [CrossRef]
26. Demény, M.A.; Virág, L. The PARP Enzyme Family and the Hallmarks of Cancer Part 1. Cell Intrinsic Hallmarks. *Cancers* **2021**, *13*, 2042. [CrossRef]
27. Livraghi, L.; Garber, J.E. PARP Inhibitors in the Management of Breast Cancer: Current Data and Future Prospects. *BMC Med.* **2015**, *13*, 188. [CrossRef]
28. Cai, Z.; Liu, C.; Chang, C.; Shen, C.; Yin, Y.; Yin, X.; Jiang, Z.; Zhao, Z.; Mu, M.; Cao, D.; et al. Comparative Safety and Tolerability of Approved PARP Inhibitors in Cancer: A Systematic Review and Network Meta-Analysis. *Pharmacol. Res.* **2021**, *172*, 105808. [CrossRef]
29. Sethi, G.S.; Dharwal, V.; Naura, A.S. Poly(ADP-Ribose)Polymerase-1 in Lung Inflammatory Disorders: A Review. *Front. Immunol.* **2017**, *8*, 1172. [CrossRef]
30. Javle, M.; Curtin, N.J. The Role of PARP in DNA Repair and Its Therapeutic Exploitation. *Br. J. Cancer* **2011**, *105*, 1114–1122. [CrossRef]
31. Morales, J.; Li, L.; Fattah, F.J.; Dong, Y.; Bey, E.A.; Patel, M.; Gao, J.; Boothman, D.A. Review of Poly (ADP-Ribose) Polymerase (PARP) Mechanisms of Action and Rationale for Targeting in Cancer and Other Diseases. *Crit. Rev. Eukaryot. Gene Expr.* **2014**, *24*, 15–28. [CrossRef]
32. Sousa, F.G.; Matuo, R.; Soares, D.G.; Escargueil, A.E.; Henriques, J.A.P.; Larsen, A.K.; Saffi, J. PARPs and the DNA Damage Response. *Carcinogenesis* **2012**, *33*, 1433–1440. [CrossRef]
33. Rose, M.; Burgess, J.T.; O'Byrne, K.; Richard, D.J.; Bolderson, E. PARP Inhibitors: Clinical Relevance, Mechanisms of Action and Tumor Resistance. *Front. Cell Dev. Biol.* **2020**, *8*, 564601. [CrossRef]
34. Zheng, F.; Zhang, Y.; Chen, S.; Weng, X.; Rao, Y.; Fang, H. Mechanism and Current Progress of Poly ADP-Ribose Polymerase (PARP) Inhibitors in the Treatment of Ovarian Cancer. *Biomed. Pharmacother.* **2020**, *123*, 109661. [CrossRef]
35. De Gaetano, G.; Tonolli, M.C.; Bertoni, M.P.; Roncaglioni, M.C. Ditazole and Platelets. *Pathophysiol. Haemost. Thromb.* **1977**, *6*, 127–136. [CrossRef]
36. Schelman, W.R.; Liu, G.; Wilding, G.; Morris, T.; Phung, D.; Dreicer, R. A Phase I Study of Zibotentan (ZD4054) in Patients with Metastatic, Castrate-Resistant Prostate Cancer. *Investig. New Drugs* **2009**, *29*, 118–125. [CrossRef]
37. Luczynski, M.; Kudelko, A. Synthesis and Biological Activity of 1,3,4-Oxadiazoles Used in Medicine and Agriculture. *Appl. Sci.* **2022**, *12*, 3756. [CrossRef]
38. Glomb, T.; Szymankiewicz, K.; Świątek, P. Anti-Cancer Activity of Derivatives of 1,3,4-Oxadiazole. *Molecules* **2018**, *23*, 3361. [CrossRef]
39. Nayak, S.; Gaonkar, S.L.; Musad, E.A.; Dawsar, A.M.A. 1,3,4-Oxadiazole-Containing Hybrids as Potential Anticancer Agents: Recent Developments, Mechanism of Action and Structure-Activity Relationships. *J. Saudi Chem. Soc.* **2021**, *25*, 101284. [CrossRef]
40. Benassi, A.; Doria, F.; Pirota, V. Groundbreaking Anticancer Activity of Highly Diversified Oxadiazole Scaffolds. *Int. J. Mol. Sci.* **2020**, *21*, 8692. [CrossRef]
41. Ren, H.; Bakas, N.A.; Vamos, M.; Chaikuad, A.; Limpert, A.S.; Wimer, C.D.; Brun, S.N.; Lambert, L.J.; Tautz, L.; Celeridad, M.; et al. Design, Synthesis, and Characterization of an Orally Active Dual-Specific ULK1/2 Autophagy Inhibitor That Synergizes with the PARP Inhibitor Olaparib for the Treatment of Triple-Negative Breast Cancer. *J. Med. Chem.* **2020**, *63*, 14609–14625. [CrossRef] [PubMed]
42. Voronkov, A.; Holsworth, D.D.; Waaler, J.; Wilson, S.R.; Ekblad, B.; Perdreau-Dahl, H.; Dinh, H.; Drewes, G.; Hopf, C.; Morth, J.P.; et al. Structural Basis and SAR for G007-LK, a Lead Stage 1,2,4-Triazole Based Specific Tankyrase 1/2 Inhibitor. *J. Med. Chem.* **2013**, *56*, 3012–3023. [CrossRef] [PubMed]
43. Puthiyapurayil, P.; Poojary, B.; Chikkanna, C.; Buridipad, S.K. Design, Synthesis and Biological Evaluation of a Novel Series of 1,3,4-Oxadiazole Bearing N-Methyl-4-(Trifluoromethyl)Phenyl Pyrazole Moiety as Cytotoxic Agents. *Eur. J. Med. Chem.* **2012**, *53*, 203–210. [CrossRef] [PubMed]
44. Strzelecka, M.; Glomb, T.; Drąg-Zalesińska, M.; Kulbacka, J.; Szewczyk, A.; Saczko, J.; Kasperkiewicz-Wasilewska, P.; Rembiałkowska, N.; Wojtkowiak, K.; Jezierska, A.; et al. Synthesis, Anticancer Activity and Molecular Docking Studies of Novel N-Mannich Bases of 1,3,4-Oxadiazole Based on 4,6-Dimethylpyridine Scaffold. *Int. J. Mol. Sci.* **2022**, *23*, 11173. [CrossRef]

45. Sun, J.; Ren, S.-Z.; Lu, X.-Y.; Li, J.-J.; Shen, F.-Q.; Xu, C.; Zhu, H.-L. Discovery of a Series of 1,3,4-Oxadiazole-2(3*H*)-Thione Derivatives Containing Piperazine Skeleton as Potential FAK Inhibitors. *Bioorganic Med. Chem.* **2017**, *25*, 2593–2600. [CrossRef]
46. Zhang, S.; Luo, Y.; He, L.-Q.; Liu, Z.-J.; Jiang, A.-Q.; Yang, Y.-H.; Zhu, H.-L. Synthesis, Biological Evaluation, and Molecular Docking Studies of Novel 1,3,4-Oxadiazole Derivatives Possessing Benzotriazole Moiety as FAK Inhibitors with Anticancer Activity. *Bioorganic Med. Chem.* **2013**, *21*, 3723–3729. [CrossRef]
47. Hamdy, R.; Ziedan, N.I.; Ali, S.; Bordoni, C.; El-Sadek, M.; Lashin, E.; Brancale, A.; Jones, A.T.; Westwell, A.D. Synthesis and Evaluation of 5-(1 H-Indol-3-Yl)-N-Aryl-1,3,4-Oxadiazol-2-Amines as Bcl-2 Inhibitory Anticancer Agents. *Bioorganic Med. Chem. Lett.* **2017**, *27*, 1037–1040. [CrossRef]
48. Sun, J.; Zhu, H.; Yang, Z.-M.; Zhu, H.-L. Synthesis, Molecular Modeling and Biological Evaluation of 2-Aminomethyl-5-(Quinolin-2-Yl)-1,3,4-Oxadiazole-2(3*H*)-Thione Quinolone Derivatives as Novel Anticancer Agent. *Eur. J. Med. Chem.* **2013**, *60*, 23–28. [CrossRef]
49. Basappa, B.; Jung, Y.Y.; Ravish, A.; Xi, Z.; Swamynayaka, A.; Madegowda, M.; Pandey, V.; Lobie, P.E.; Sethi, G.; Ahn, K.S. Methyl-Thiol-Bridged Oxadiazole and Triazole Heterocycles as Inhibitors of NF-κB in Chronic Myelogenous Leukemia Cells. *Biomedicines* **2023**, *11*, 1662. [CrossRef]
50. Sebastian, A.; Pandey, V.; Mohan, C.D.; Chia, Y.T.; Rangappa, S.; Mathai, J.; Baburajeev, C.P.; Paricharak, S.; Mervin, L.H.; Bulusu, K.C.; et al. Novel Adamantanyl-Based Thiadiazolyl Pyrazoles Targeting EGFR in Triple-Negative Breast Cancer. *ACS Omega* **2016**, *1*, 1412–1424. [CrossRef]
51. Dukanya; Shanmugam, M.K.; Rangappa, S.; Metri, P.K.; Mohan, S.; Basappa; Rangappa, K.S. Exploring the Newer Oxadiazoles as Real Inhibitors of Human SIRT2 in Hepatocellular Cancer Cells. *Bioorganic Med. Chem. Lett.* **2020**, *30*, 127330. [CrossRef]
52. Malojirao, V.H.; Girimanchanaika, S.S.; Shanmugam, M.K.; Sherapura, A.; Dukanya; Metri, P.K.; Vigneshwaran, V.; Chinnathambi, A.; Alharbi, S.A.; Rangappa, S.; et al. Novel 1,3,4-Oxadiazole Targets STAT3 Signaling to Induce Antitumor Effect in Lung Cancer. *Biomedicines* **2020**, *8*, 368. [CrossRef]
53. Vishwanath, D.; Girimanchanaika, S.S.; Dukanya, D.; Rangappa, S.; Yang, J.-R.; Pandey, V.; Lobie, P.E.; Basappa, B. Design and Activity of Novel Oxadiazole Based Compounds That Target Poly(ADP-Ribose) Polymerase. *Molecules* **2022**, *27*, 703. [CrossRef]
54. Ma, H.-Y.; Zha, Z.-G.; Zhang, Z.-L.; Meng, L.; Wang, Z.-Y. Electrosynthesis of Oxadiazoles from Benzoylhydrazines. *Chin. Chem. Lett.* **2013**, *24*, 780–782. [CrossRef]
55. Haines, B.E.; Steussy, C.N.; Stauffacher, C.V.; Wiest, O. Molecular Modeling of the Reaction Pathway and Hydride Transfer Reactions of HMG-CoA Reductase. *Biochemistry* **2012**, *51*, 7983–7995. [CrossRef]
56. Lu, F.; Gong, F.; Li, L.; Zhang, K.; Li, Z.; Zhang, X.; Yin, Y.; Wang, Y.; Gao, Z.; Zhang, H.; et al. Electrochemical Synthesis of 2,5-Disubstituted 1,3,4-Oxadiazoles from α-Keto Acids and Acylhydrazines under Mild Conditions. *Eur. J. Org. Chem.* **2020**, *2020*, 3257–3260. [CrossRef]
57. Dolman, S.J.; Gosselin, F.; O'Shea, P.D.; Davies, I.W. Superior Reactivity of Thiosemicarbazides in the Synthesis of 2-Amino-1,3,4-Oxadiazoles. *J. Org. Chem.* **2006**, *71*, 9548–9551. [CrossRef]
58. Baburajeev, C.P.; Dhananjaya Mohan, C.; Ananda, H.; Rangappa, S.; Fuchs, J.E.; Jagadish, S.; Sivaraman Siveen, K.; Chinnathambi, A.; Ali Alharbi, S.; Zayed, M.E.; et al. Development of Novel Triazolo-Thiadiazoles from Heterogeneous "Green" Catalysis as Protein Tyrosine Phosphatase 1B Inhibitors. *Sci. Rep.* **2015**, *5*, 14195. [CrossRef]
59. Singh, S.; Sharma, L.K.; Saraswat, A.; Siddiqui, I.R.; Kehri, H.K.; Singh, R.K.P. Electrosynthesis and Screening of Novel 1,3,4-Oxadiazoles as Potent and Selective Antifungal Agents. *RSC Adv.* **2013**, *3*, 4237. [CrossRef]
60. Basappa, B.; Chumadathil Pookunoth, B.; Shinduvalli Kempasiddegowda, M.; Knchugarakoppal Subbegowda, R.; Lobie, P.E.; Pandey, V. Novel Biphenyl Amines Inhibit Oestrogen Receptor (ER)-α in ER-Positive Mammary Carcinoma Cells. *Molecules* **2021**, *26*, 783. [CrossRef]
61. Huey, R.; Morris, G.M.; Olson, A.J.; Goodsell, D.S. A Semiempirical Free Energy Force Field with Charge–Based Desolvation. *J. Comput. Chem.* **2007**, *28*, 1145–1152. [CrossRef] [PubMed]
62. Sulaiman, N.B.; Mohan, C.D.; Basappa, S.; Pandey, V.; Rangappa, S.; Bharathkumar, H.; Kumar, A.P.; Lobie, P.E.; Rangappa, K.S. An azaspirane derivative suppresses growth and induces apoptosis of ER-positive and ER-negative breast cancer cells through the modulation of JAK2/STAT3 signaling pathway. *Int. J. Oncol.* **2016**, *49*, 1221–1229. [CrossRef] [PubMed]
63. Bharathkumar, H.; Mohan, C.D.; Ananda, H.; Fuchs, J.E.; Li, F.; Rangappa, S.; Surender, M.; Bulusu, K.C.; Girish, K.S.; Sethi, G.; et al. Microwave-assisted synthesis, characterization and cytotoxic studies of novel estrogen receptor α ligands towards human breast cancer cells. *Bioorg. Med. Chem. Lett.* **2015**, *25*, 1804–1807. [CrossRef] [PubMed]
64. Blanchard, V.; Chevalier, F.; Imberty, A.; Leeflang, B.R.; Basappa; Sugahara, K.; Kamerling, J.P. Conformational studies on five octasaccharides isolated from chondroitin sulfate using NMR spectroscopy and molecular modeling. *Biochemistry* **2007**, *46*, 1167–1175. [CrossRef]
65. Basappa; Rangappa, K.S.; Sugahara, K. Roles of glycosaminoglycans and glycanmimetics in tumor progression and metastasis. *Glycoconj. J.* **2014**, *31*, 461–467. [CrossRef]
66. Kumar, C.A.; Jayarama, S.; Basappa; Salimath, B.P.; Rangappa, K.S. Pro-apoptotic activity of imidazole derivatives mediated by up-regulation of Bax and activation of CAD in Ehrlich Ascites Tumor cells. *Investig. New Drugs* **2007**, *25*, 343–350. [CrossRef]
67. BIOVIA Dassault Systèmes. *Discovery Studio Visualizer*; 21.1.0.20298; Dassault Systèmes: San Diego, CA, USA, 2020.
68. Schrödinger, L.L.C.; DeLano, W. PyMOL. 2020. Available online: http://www.pymol.org/pymol (accessed on 15 February 2023).

69. Pettersen, E.F.; Goddard, T.D.; Huang, C.C.; Couch, G.S.; Greenblatt, D.M.; Meng, E.C.; Ferrin, T.E. UCSF Chimera—A Visualization System for Exploratory Research and Analysis. *J. Comput. Chem.* **2004**, *25*, 1605–1612. [CrossRef]
70. Frisch, M.J.; Trucks, G.W.; Schlegel, H.B.; Scuseria, G.E.; Robb, M.A.; Cheeseman, J.R.; Scalmani, G.; Barone, V.; Mennucci, B.; Petersson, G.A.; et al. *Gaussian09, Revision D.01*; Gaussian, Inc.: Wallingford, CT, USA, 2009.